SNR-Improvement of Four-Wave-Mixing Wavelength Converters using Raman Amplification

Frederik Klejs[(1)*], Lukasz Krzczanowicz[(1)], Deming Kong[(1)], Michael Galili[(1)], Yabin Ye[(2)], Leif K. Oxenløwe[(1)]

[(1)] DTU Fotonik, Department of Photonics Engineering, Technical University of Denmark
[(2)] Munich Research Center, Huawei Technologies Duesseldorf GmbH
*frek@fotonik.dtu.dk

Based on a detailed experimental data-quality analysis of a FWM wavelength converter based on highly nonlinear fibres, we find significant improvement potentials, and demonstrate >1-dB SNR improvement of a converted 16-QAM, 32-Gbaud data signal by adding Raman amplification to the FWM process.

Introduction

All-optical wavelength converters offer increased flexibility of optical networks by enabling WDM channels to be moved to different wavelength slots, e.g. allowing for more efficient and faster routing through networks and enhance networking possibilities in passive optical networks Covering e.g., the full C-band may necessitate dual-stage converters for full conversion flexibility[1], but this increases the sensitivity to conversion losses, owing to conversion efficiencies less than unity. Fibre-based wavelength converters (WC) are attractive, as they offer the highest reported conversion efficiencies[2]. However, fibre based wavelength converters are limited by stimulated Brillouin scattering (SBS), keeping the tolerable pump power low, or requiring pump modulation schemes, which in turn makes it incompatible with some phase-dependent data signals. Using Raman amplification to enhance nonlinear processes in fibre has been reported previously[3], but the added complexity and possible ASE-impact on the overall system have raised concerns.

In this work we present a detailed experimental investigation of a Raman-assisted four-wave mixing (R-a FWM) wavelength converter, where the data quality of the converted signal is measured in terms of the signal-to-noise ratio (SNR) of the received bit pattern of a 32-Gbaud 16-QAM data signal. The analysis reveals, for the first time, new optimum settings for highly nonlinear fibre (HNLF) based wavelength converters, yielding up to 4 dB higher conversion efficiencies, and >1dB higher SNR of the received converted data signal. Thus, adding a Raman pump to the converter offers a real total subsystem improvement, by allowing one to remain below the SBS threshold for the FWM-pump, whilst not impairing the signal by Raman ASE.

Experimental Setup

The FWM takes place in a HNLF, a SPINE (Stable Phase-matching for Improved Nonlinear Efficiency) fiber with a zero-dispersion wavelength of 1545.9 nm made by OFS, and the FWM pump is placed at the optimal wavelength (1545.9 nm). The Raman pump is at 1452 nm. The signal and FWM pump are combined using a 10-dB coupler, with the attenuated arm used for the signal to emulate loss due to transmission. coupler, to minimize the coupling loss, and is decoupled again after passing through the HNLF. The Raman pump is launched counter propagation-wise in the fiber, as that lessens the presence of the Raman pump ASE noise at the output of the WC. A low-noise preamplifier is used for the signal, whereas a high power amplifier is used for the FWM pump.

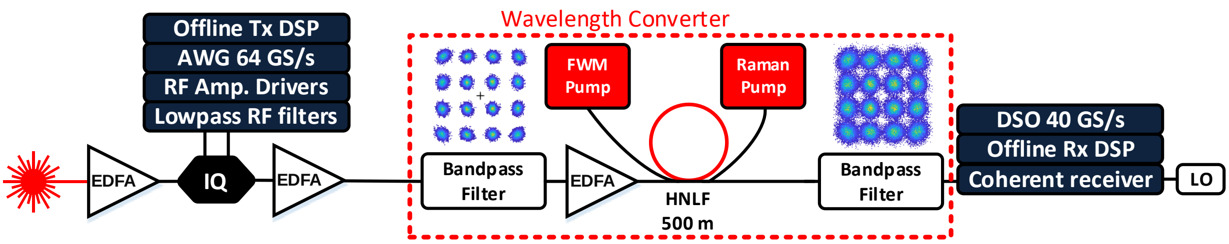

Fig. 1: The experimental setup, The highly nonlinear fiber (HNLF) used is a SPINE fiber designed for high conversion efficiencies. The signal and four-wave-mixing pump were combined using a 90/10 coupler and the Raman pump was added using a WDM-coupler. For the power measurements an OSA was used instead of the receiver.

978-1-6654-3868-1/21/$31.00 ©2021 IEEE

The Raman pump is added using a WDM-The Raman and FWM pump powers are swept through various regimes to characterize the effect on the converted signal's SNR. The signal power launched into the HNLF is 0 dBm, and the FWM pump power is varied between 17.5 and 27 dBm. A single polarization 16-QAM, 32 Gbaud signal at 1551 nm is used to characterize the R-a FWM unit's performance. After conversion the converted signal (idler) is filtered out and sent to the receiver. In the receiver we have an additional filter followed by an EDFA operated at constant output power. To detect and analyze the received idler we use a coherent receiver employing off-line digital signal processing (DSP). The DSP uses an adaptive equalizer and 4% pilot symbols, the SNR of the pilot symbols is evaluated separately, so as to not artificially increase the SNR. The SNR of the received idler is calculated by comparing the equalized and phase recovered symbols with the sent symbols, using 3 traces, each of 130.000 data symbols. Errorbars are calculated by finding the for parts of a trace and then calculating the standard deviation. SNR is chosen because it includes all impairments to the signal, both linear and non-linear noise. Had we only used conversion efficiency (CE), we would not see the effect of SBS on the phase noise of the converted signal, and we might have concluded that pump powers beyond 27 dBm would be optimal. The power measurements of the pump power, idler power and OSNR measurements are made using an OSA with a resolution of 0.1 nm. We scanned between 1535- and 1555 nm and compared the spectra.

Noise Figure and Conversion Efficiency

The noise figure of the wavelength converter can be determined from the conversion efficiency (CE) of the FWM process. Firstly the noise figure can be derived by considering the FWM wavelength converter a parametric amplifier with negative gain, and can be determined by the CE[5], seen in Eq. (1). It can be shown that the gain of an optical parametric amplifier is related to the CE (η) via Eq. (2). Combining these observations we can construct an expression for the noise figure of a wavelength convertor based on the CE. Using the Friis formula for a system of cascaded components[6] we can find the total noise figure, Eq.(3), of a system consisting of two EDFAs with a WC in between.

$$NF_{idler} = \frac{2G}{G-1} \qquad (1)$$

$$G = \eta + 1, \qquad NF_{idler} = \frac{2+2\eta}{\eta} \qquad (2)$$

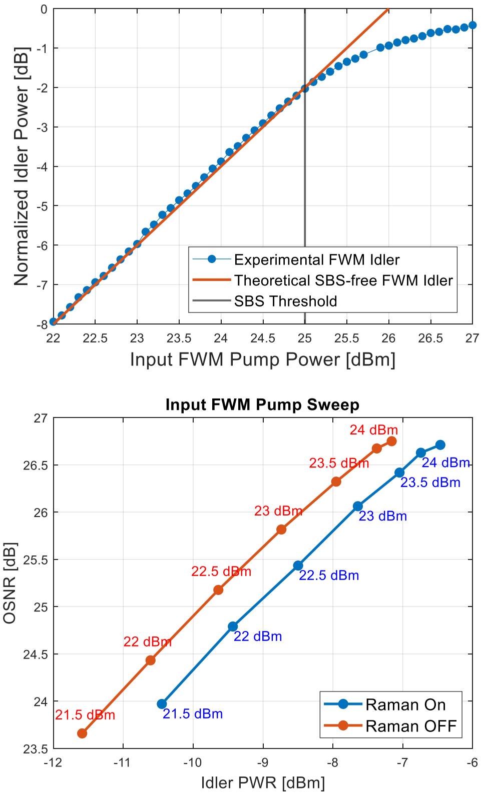

Fig.2A (Top): Normalized idler power versus FWM pump power. The orange line has the expected slope of 2 for ideal SBS-free FWM. The vertical line points to the SBS threshold for the FWM pump power. **Fig. 2B (Bottom):** OSNR vs idler power with and without Raman amplification in the fiber. The numbers refer to the corresponding FWM pump power. Adding Raman amplification increases the idler power and OSNR for a given FWM pump setting.

$$F_{total} = F_{EDFA} + \frac{2+2\eta-\eta}{\eta G_{EDFA}} + \frac{F_{EDFA2}-1}{(1+\eta)G_{EDFA}} \qquad (3)$$

Plotting these equations, as in Fig.3, it can be shown that once a system reaches a CE of ≈ -10 dB, further increasing the CE yields little improvement in the overall noise figure. This number is also reported on in other work[1].

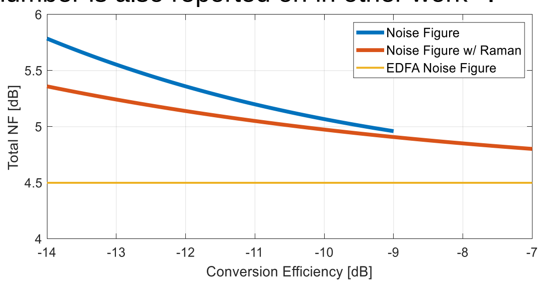

Fig.3: Noise figure for a system of two EDFAs with a wavelength conversion stage in between. Once the system reaches -10 dB CE, further increasing the CE yields little effect.

This goes to show that increasing the CE of a wavelength converter reduces the noise figure, and that increasing the CE far beyond -10 dB brings little extra yield. So, a -10 dB CE is a good target for a low NF wavelength converter. As

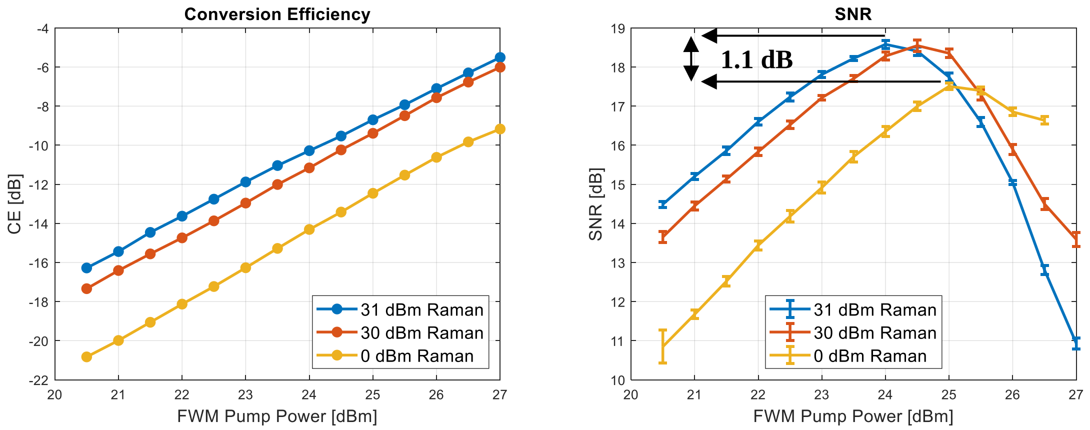

Fig. 4A(Left): The conversion efficiency of the four-wave-mixing process as a function of the input four-wave-mixing pump power. **Fig. 4B(Right):** The signal-to-noise ratio of the received idler data signal as a function of the FWM pump power.

seen in Fig. 2 below, using R-a FWM greatly improves the CE, and R-a FWM is thus a good candidate for low-NF wavelength converters.

Results and Discussion

Fig. 2A shows the normalized output idler power vs the input FWM pump power, revealing an SBS threshold at 25 dBm FWM pump power. The optimal FWM pump power is marked with a vertical line, above which the measured FWM idler deviates from the theoretical ideal SBS-free FWM curve. The idler power increases further as we increase the pump power, however the signal quality will deteriorate, due to the nonlinear noise caused by SBS, which is only captured by measuring the SNR, as seen in Fig. 4B, and not even by measuring the OSNR, as seen in Fig. 2B, which shows the OSNR vs the output idler power. The numbers in the figure indicates the FWM pump power used to generate the idler. For a given FWM pump power, we see that both the OSNR and the idler power increase when we add the Raman pump to the FWM process. The increase in idler power, however, is larger than the increase in OSNR, due to the additional Raman ASE.

Fig. 4A shows the CE versus the input FWM pump power. Without the Raman pump the CE reaches -9.2 dB input-to-output CE at maximum available FWM pump power coupled into the HNLF. Dithering could be used to mitigate the SBS however this would transfer the dithering to the idler which is an issue for network applications, unless a counter-dithering scheme is used[8], which could still leave a mark on the phase of the idler. Adding the Raman pump the CE at max-FWM pump reaches -6 dB. Increasing the power of the Raman pump, from 30 dBm to 31 dBm, increases this gain by 0.5 dB at max-FWM pump and nearly 1 dB at lower FWM pump power, yielding gains of up to 4 dB.

Fig. 4B shows the received SNR vs the FWM pump power, with and without Raman, at two different Raman pump powers. The cases with Raman reach the highest SNR, of around 18.6 dB, vs only 17.5 dB SNR attained without Raman. Additionally, it is clearly observed that there is an optimum, unlike for the CE-case on Fig 4A. This is because the SBS influence on the data signal is picked up by the SNR measurement. The optimum SNR is obtained for lower FWM pump power in the Raman cases, i.e. below the SBS threshold, which helps to give a higher SNR. It is worth noting that the cases with Raman operates at the optimal SNR around -10 dB CE, whereas the optimum case without Raman operates at -12 dB CE, at 25 dBm FWM pump power. We therefore infer that the 2 dB increase in CE leads to a >1-dB increase in the received SNR after wavelength conversion.

Conclusions and Outlook

We have, for the first time, extensively characterized a wavelength conversion system using Raman amplification to enhance the nonlinear FWM process. We have shown that ultimately no penalties are encountered when including the Raman amplification in the system, and that the noise from the Raman pump is more compensated by the increased CE. We successfully demonstrated the wavelength conversion and decoding of a single polarization 16-QAM, 32 Gbaud signal. We showed a 2 dB increase in the CE of the system leading to a 1.1 dB improvement of the SNR when we included Raman amplification in the HNLF to enhance the FWM process. Further work includes investigating more sophisticated pump configurations of the Raman pumps, possibly using more than a single Raman pump [7].

Acknowledgements

Thanks to Huawei for sponsoring this work, the SPOC centre (DNRF-123) for infrastructure, and OFS Denmark ApS for the SPINE fibre.

References

[1] H. Nguyen Tan *et al*, ”On the Cacadeability of All-Optical Wavelength Converter of High-Order QAM formats”, *Journal of Lightwave Tech.,* vol. 34, pp. 3194-3205, 2016.

[2] T. Torounidis *et al*, “Fiber Parametric Amplifier with 70-dB Gain”, *IEEE Photon. Technol. Lett.,* vol. 18, no. 10, pp. 1194-1196, 2006.

[3] Quang Le N.T. *et al*, ”Enchancement of Non-linear response of a highly non-linear fibre due to Raman amplification”, in Proc. of the European Conf. on Opt. Communications (ECOC), 2002.

[4] P. Kaminski *et al,*”Unrepeatered transmission reach extension by receiver-side all optical back-propagation”, in Proc. of OptoElectronics and Communications Conference (OECC), 2019.

[5] P. Kylemark *et al*, “Noise Characteristics of Fiber Optical Parametric Amplfiers”, *Journal of Lightwave Tech*, vol. 22, pp. 409-416, Feb 2004.

[6] D.M. Baney, “Theory and Measurement Techniques for the Noise Figure of Optical Amplifiers”, *Opt. Fiber Tech.,* vol. 6, pp. 122-154, 2000

[7] Ania-Castañón, Juan Diego. "Quasi-lossless transmission using second-order Raman amplification and fibre Bragg gratings." *Optics Express,* vol. 12, no. 19, pp. 4372-4377, 2004